

# A Novel Member of the Netrin Family, $\beta$ -Netrin, Shares Homology with the $\beta$ Chain of Laminin: Identification, Expression, and Functional Characterization

Manuel Koch,\* Julie R. Murrell,<sup>‡</sup> Dale D. Hunter,<sup>‡§||</sup> Pamela F. Olson,<sup>\*||</sup> William Jin,\* Douglas R. Keene,\*\* William J. Brunken,<sup>\*¶</sup> and Robert E. Burgeson\*

\*Cutaneous Biology Research Center, Massachusetts General Hospital, Harvard Medical School, Charlestown, Massachusetts 02129;

<sup>‡</sup>Department of Neuroscience, <sup>§</sup>Department of Anatomy and Cell Biology, and <sup>||</sup>Department of Ophthalmology, Tufts University

School of Medicine, Boston, Massachusetts 02111; <sup>¶</sup>Department of Biology, Boston College, Chestnut Hill, Massachusetts 02467; and

\*\*Shriners Hospital for Children, Portland, Oregon 97201

**Abstract.** The netrins are a family of laminin-related molecules. Here, we characterize a new member of the family,  $\beta$ -netrin.  $\beta$ -Netrin is homologous to the NH<sub>2</sub> terminus of laminin chain short arms; it contains a laminin-like domain VI and 3.5 laminin EGF repeats and a netrin C domain. Unlike other netrins, this new netrin is more related to the laminin  $\beta$  chains, thus, its name  $\beta$ -netrin. An initial analysis of the tissue distribution revealed that kidney, heart, ovary, retina, and the olfactory bulb were tissues of high expression. We have expressed the molecule in a eukaryotic cell expression system and made antibodies to the expressed product. Both in situ hybridization and immunohistochemistry were used to describe the cellular source of  $\beta$ -netrin

and where  $\beta$ -netrin is deposited.  $\beta$ -Netrin is a basement membrane component; it is present in the basement membranes of the vasculature, kidney, and ovaries. In addition,  $\beta$ -netrin is expressed in a limited set of fiber tracts within the brain, including the lateral olfactory tract and the vomeronasal nerve. Functional studies were performed and show that  $\beta$ -netrin promotes neurite elongation from olfactory bulb explants. Together, these data suggest that  $\beta$ -netrin is important in neural, kidney, and vascular development.

**Key words:** axon guidance • kidney • olfactory bulb • vasculature • brain

## Introduction

Netrins comprise a family of structurally related secreted molecules involved in axon guidance. Axons sense netrins as either attractants or repellents, depending upon which netrin receptors are expressed on their growth cones (Hedgecock et al., 1990; Serafini et al., 1994; Colamarino and Tessier-Lavigne, 1995; Winberg et al., 1998) or differences in the cellular signal transduction machinery (Bashaw and Goodman, 1999).

To date, several netrins have been described. A single netrin, UNC-6, has been identified in *Caenorhabditis elegans* (Ishii et al., 1992) and two have been described in *Drosophila*, Netrin-A and Netrin-B (Harris et al., 1996; Mitchell et al., 1996). Three netrins have been identified in vertebrates: netrin-1 has been identified in chicken (Serafini et al., 1994), mouse (Serafini et al., 1996), *Xenopus* (de la Torre et al., 1997), zebrafish (Lauderdale et al., 1997;

Strahle et al., 1997), and humans (Meyerhardt et al., 1999); netrin-2 in chickens (Serafini et al., 1994); and netrin-3 in humans (NTN2L; Van Raay et al., 1997) and mouse (Wang et al., 1999). Netrins 1, 2, and 3 are all structurally related to the short arms of laminin  $\gamma$  chains, and contain a laminin VI domain and three EGFlike repeats similar to the laminin V domain (V-1, V-2, and V-3); they also contain a positively charged heparin-binding COOH-terminal domain termed domain C (Serafini et al., 1994; Keino-Masu et al., 1996).

Mutations in the netrin genes in *C. elegans* (*unc-6*) (Hedgecock et al., 1990), *Drosophila* (NetA/B) (Winberg et al., 1998), and mouse (netrin-1) (Skarnes et al., 1995; Serafini et al., 1996) produce defects in axon guidance affecting circumferential and commissural growth. Studies in vitro show that netrin-1 can act from a distance within a collagen gel to cause the outgrowth of spinal cord axons, implicating chemoattraction as one of the mechanisms of action of netrins (Kennedy et al., 1994).

In the mouse and chicken, the RNA transcripts encoding the netrins are widely distributed throughout the organism

Address correspondence to R.E. Burgeson, CBRC MGH-East Building 149, Charlestown, MA 02129. Tel.: (617) 726-4186. Fax: (617) 726-4453. E-mail: bob.burgeson@cbrc2.mgh.harvard.edu

Pamela F. Olson's current address is Department of Ophthalmology, Tufts University School of Medicine, Boston, MA 02111.

(Wang et al., 1999). Netrin RNAs are prominent in embryonic muscle and the bronchi of lung; transcripts are also present in the condensing mesenchyme of the limb and esophagus. However, netrin RNA location has been most extensively documented in the central nervous system (CNS)<sup>1</sup>: netrin-1 is strongly expressed in the developing spinal cord, in the floorplate, and the ventral ventricular zone (Serafini et al., 1996; Puschel, 1999; Wang et al., 1999); netrin-2 is expressed throughout the spinal cord and in the dorsal root ganglia, but not in the floorplate (Wang et al., 1999); and netrin-3 is expressed in sensory (dorsal root and cranial) ganglia (Puschel, 1999; Wang et al., 1999).

The effect of netrins upon axon extension in vitro, together with the tightly restricted regional expression of netrin RNAs within targets of axon outgrowth, support the generally held hypothesis that netrins act as diffusible attractants or repellents for responsive axons. However, localization of netrin-1 protein in the chicken brain, retina, and spinal cord appear to contradict this concept (MacLennan et al., 1997). For example, in the spinal cord, although netrin-1 RNA is localized where the commissural fibers cross in the floorplate, netrin-1 protein is not concentrated within the floorplate. Rather, netrin-1 protein is deposited in or near the basement membrane of the spinal cord. Similarly, Netrin-A and Netrin-B proteins are localized at the *Drosophila* midline in a manner analogous to that in the chicken spinal cord (Harris et al., 1996). The ability of the netrins to bind heparin through the C domain (Serafini et al., 1994; Keino-Masu et al., 1996) is consistent with a haptotactic function for netrins (MacLennan et al., 1997), as this binding suggests that netrins may be immobilized in tissues, either to cell surfaces or to components of the extracellular matrix. Here, we describe another member of the netrin family in humans and mice. Netrins-1, 2, and 3, while containing some laminin  $\beta$  chain-like features (Ishii et al., 1992; Wadsworth et al., 1996), are more closely related to the laminin  $\gamma$  chains than to other laminin chains. In contrast, the novel netrin, described here, is more closely related to laminin  $\beta$  chains than to other laminin short arms. Hence, we have termed this molecule  $\beta$ -netrin.

## Materials and Methods

### cDNA Isolation

Comparison of the laminin  $\beta 2$  chain amino acid sequence (SWISS-PROT accession number NP\_002283) with the dbEST database (Boguski, et al., 1993; National Center for Biotechnology Information) using the program BLAST (Altschul et al., 1990) yielded one clone (EMBL/Genbank/DDBJ accession number Z50158) as a possible candidate for a novel laminin chain. Specific primers for 5' or 3' extensions were deduced from that expressed sequence tag, and nested PCRs were performed on skeletal muscle cDNA or human placental cDNA to extend the clone using Marathon-Ready cDNA (CLONTECH Laboratories, Inc.) following the manufacturer's instructions. For PCR, the Long Expand PCR Kit (Boehringer Mannheim) was used with the following conditions: denaturation, 94°C for 3 min; 10 cycles of 94°C for 30 s, 63°C (−0.5°C per cycle) for 30 s, and 68°C for 4 min; 25 cycles of 94°C for 30 s, 58°C for 30 s, and 68°C for 4 min (+10 s per cycle); and a final extension period at 68°C of 8 min.

The PCR samples from the first round were purified (PCR purification kit; QIAGEN) and 2% of the sample volume was used in the second round of PCR using the PCR protocol given above. These PCR products were purified from an agarose gel (gel purification kit™; QIAGEN) and

either subcloned (into PCR II or PCR 2.1 vectors; Invitrogen) or directly used for sequencing. To confirm the nucleotide sequence and control for PCR-induced nucleotide substitutions, gene-specific primers were used to re-amplify the entire cDNA. A first strand cDNA synthesis kit (CLONTECH Laboratories, Inc.) was used to synthesize cDNA from total spleen RNA using oligo dT or random primers following the manufacturer's protocol; PCR was used to generate overlapping clones complementary to the entire human  $\beta$ -netrin. Sequencing of all the PCR products obtained from the cDNA confirmed the nucleotide sequence of the human  $\beta$ -netrin.

To clone the mouse  $\beta$ -netrin, nested PCR was performed on reverse-transcribed embryonic day 15.5 (E15.5) mouse RNA using, for the first PCR round, the primers Fv1 (5'-dCTGAAACGACAGTCTTGTC-CCTG-3') and Rv1 (5'-dTAAATGTCTGTTCTTACTTTCGCA-3'), and, for the second PCR round, nested primers Nfv2 (5'-dCATTGT-CAAGGGCAGCTGCTTCTG-3') and NRv2 (5'-dGCCACCCAG-GCTTGCAAGGGCA-3'). The PCR conditions were as follows: 1 U *Taq* polymerase (Fisher Scientific); denaturation, 94°C for 3 min; 10 cycles of 94°C for 30 s, 50°C (−0.5°C per cycle) for 30 s, and 72°C for 1 min; 25 cycles of 94°C for 30 s, 60°C for 30 s, and 72°C for 1 min; and a final extension period at 72°C of 5 min. The 500-bp PCR product was purified on an agarose gel and directly sequenced. The sequence information was used to generate primers that were used in nested PCR using embryonic day 17 (E17) mouse cDNA (Marathon-Ready) to elongate the 3' and 5' ends of the mouse  $\beta$ -netrin cDNA.

To generate a genetic relationship map of the netrins and laminins, the NH<sub>2</sub> termini of protein sequences were analyzed with the GrowTree program (SeqWeb; Genetics Computer Group Inc.); the following laminin and netrin protein sequences were used: netrin-1 (AF128865); netrin 3 (AF128866); laminin  $\alpha 1$  chain (J04064); laminin  $\alpha 2$  chain (MMU12147); laminin  $\beta 1$  chain (M15525); laminin  $\beta 2$  chain (AH006792); laminin  $\beta 3$  chain (U43298); laminin  $\gamma 1$  chain (J03484); and laminin  $\gamma 3$  chain (AF079520). Protein sequence starting from the VI domain through the three laminin-EGF modules in domain V were analyzed. The Jukes-Cantor method was chosen to correct the distances for multiple substitutions at a single site; the tree was created with the unweighted pair group method using arithmetic averages (UPGMA) algorithm.

### Nucleotide Sequencing

Nucleotide sequences were determined with a Thermo Sequenase cycle sequencing kit and <sup>33</sup>P-ddNTPs (Amersham Pharmacia Biotech) using either M13 forward or reverse primers or gene-specific primers synthesized in our laboratory. A 1.5:1 ratio of inosine to guanosine was included in the sequencing mix. Sequence data were assembled and manipulated using Genetyx-Max 8.0 and Genestream-1 at <http://www2.igh.cnrs.fr/> (Software Development Co., Ltd.). The signal peptide cleavage site was predicted using: <http://genome.cbs.dtu.dk/services/SignalP/> (Nielsen et al., 1997).

### Northern and Dot Blot Analyses

A 1.7-kbp PCR product (nucleotides 1,114–2,946) was labeled with <sup>33</sup>P-dCTP (NEN Life Science Products) using the *rediprime* DNA labeling system (Amersham Pharmacia Biotech). Northern and dot blots (CLONTECH Laboratories, Inc.) were prehybridized in 50% formamide, 5× SSPE, 1× Denhardt's, 1% SDS, 10% dextran-sulfate, and 0.1 mg/ml salmon sperm DNA (GIBCO BRL) at 42°C for 2 h. Without further purification, the probe was denatured in the same buffer plus 1/10 vol/vol human Cot-1 DNA (Boehringer Mannheim), and 1/10 vol/vol sheared salmon testis DNA (GIBCO BRL) at 94°C for 5 min, placed on ice, added to the blots, and was hybridized for 20 h. Blots were washed three times in 2× SSC, 1% SDS at 42°C and two times in 0.1× SSC, 1% SDS at 42°C. Blots were placed on BioMax MR film with a BioMax TranScreen-LE intensifying screen (both from Eastman Kodak Co.) for 20 h at −70°C.

### Reverse Transcriptase-PCR (RT-PCR) on Tissue RNA

RNA was isolated from animal tissues using the RNeasy kit (QIAGEN), and cDNA was reverse-transcribed using an RT-PCR kit (CLONTECH) from the isolated RNA. PCR was performed on these cDNAs using a long expand PCR kit (Boehringer Mannheim) with GAPDH primers (forward: 5'-pTGAAGGTCGGTGTGAACGGA-3'; reverse: 5'-dGATGGCATGCACTGTGGTCA-3') and the amount of template was normalized for each tissue. A range of cycle numbers was tested to ensure the amounts were normalized in the linear range of the reaction. With the gene-specific primers (forward: 5'-dGTAAGCCCGTTTCTACCGGACC-3'; reverse: 5'-dCCCTTGTGTGCTTAAGACCTTACG-3'), another PCR was performed with the normalized cDNA templates using the following con-

<sup>1</sup>Abbreviations used in this paper: CNS, central nervous system; r $\beta$ -N, recombinant mouse  $\beta$ -netrin; RT-PCR, reverse transcriptase-PCR.

ditions: denaturation, 2 min; 94°C, 10 cycles of 94°C for 30 s, 65°C (−0.5°C per cycle) for 30 s, and 68°C for 2 min; 22 cycles of 94°C for 30 s, 60°C for 30 s, and 68°C for 2 min (+10 s per cycle); and a final extension period at 68°C for 5 min. A pair of gene-specific primers was selected from four pairs, which were each tested on the cDNAs for optimal amplification/cycle number. PCR products were confirmed by sequencing.

### Recombinant Expression of Secreted Proteins

The following fragments of laminin chain cDNAs were amplified by PCR and subcloned into an episomal expression vector: human laminin  $\gamma$ 2 short arm (Amano et al., 2000); mouse laminin  $\gamma$ 3 short arm (AF079520), nucleotides 1–3,122; and mouse laminin  $\beta$ 2 short arm (NM\_008483), nucleotides 174–3,659. The following full lengths or fragments of the netrin coding sequences were similarly obtained: mouse netrin-1 (U65418), nucleotides 46–1,812; mouse  $\beta$ -netrin (AF278532), nucleotides 311–2,143; and mouse  $\beta$ -netrin- $\Delta$ C (AF278532), nucleotides 311–1,672. 1  $\mu$ g of the total RNA from whole mouse embryo (day 17) was reverse transcribed, and the PCR was performed following the manufacturer's instructions (*Pfu* Turbo DNA polymerase; Stratagene). The PCR product was purified on an agarose gel (QIAGEN) and subcloned (rapid DNA ligation kit; Roche Diagnostics GmbH) into a modified PCEP-4 (gift from Ernst Poeschl, Munich, Germany) expression vector. For convenience, a six histidine tag followed by a stop codon was introduced at the 3' end of the laminin  $\gamma$ 2 and  $\gamma$ 3 chains sequences adjacent to the BamHI site of the PCEP-4 vector, and a six histidine tag followed by a thrombin cleavage site was included adjacent to the NheI site of the  $\beta$ -netrin, netrin-1, and laminin  $\beta$ 2 chain sequences. The ligated DNA was transformed into TOP 10 cells (Invitrogen). Plasmids were isolated from bacteria (QIAGEN) and sequenced with gene-specific primers (Thermo Sequenase cycle sequencing kit; Amersham Pharmacia Biotech). In the case of the netrin-1 clone, we detected a single amino acid substitution V to L at position nucleotides 295–297 (present in all the sequenced clones, each of which were independent PCR products). 293-EBNA cells (Invitrogen) were transformed (FuGene; Roche Diagnostics GmbH) with the expression vector and selected after 2 d with puromycin (Sigma-Aldrich).

Stably transfected 293-EBNA cells were subcloned and the highest protein producing clones were expanded for large-scale production. 2 liters of supernatant from these cells was collected and supplemented with 0.5 mM PMSF. After ammonium sulfate precipitation (45%), the precipitate was collected by centrifugation and dialyzed against the binding buffer (200 mM NaCl and 20 mM Tris-HCl, pH 8). The dialyzed protein was applied onto a nickel-chelated Sepharose column (Amersham Pharmacia Biotech) and washed and eluted with binding buffer containing increasing concentrations of imidazole (10–80 mM imidazole). In some cases, the histidine tag was digested with thrombin (isolated from bovine plasma; Sigma-Aldrich) according to the protocol from Novagen Inc. The digested protein was again applied to a nickel-chelated Sepharose column and eluted with increasing imidazole concentration. The protein was dialyzed against PBS and the protein concentration was determined according to the protocol from Whitaker and Granum (1980). Rotary shadowing was performed using our previously published methods (Rousselle et al., 1997).

### Antibody Production

The  $\beta$ -netrin fusion protein  $\beta$ -N was injected intradermally into a rabbit (R33) and mice for antibody production following standard procedures (Harlow and Lane, 1988). The R33 antiserum was purified over a protein G column (Amersham Pharmacia Biotech) and eluted with triethylamine (Sigma Chemical Co.). The neutralized eluate was affinity-purified by applying it to a mouse  $\beta$ -netrin fusion protein column. To prepare this column, full-length recombinant  $\beta$ -netrin, from which the His tag was removed, was coupled to activated CNBr-Sepharose. Bound antibodies were eluted with triethylamine and immediately neutralized. From the hybridoma screen, two positive clones producing mAbs against  $\beta$ -netrin were identified: 9F11, which our studies show is conformation-sensitive (data not shown), and 61.

### Immunohistochemistry and In Situ Hybridization

Mice and rats were killed according to protocols approved by institutional animal care committees. Immunohistochemistry was performed as previously described (Libby et al., 1997; Koch et al., 1999). Adult tissues were embedded in OCT compound (Miles, Elkhart, IN) and frozen by immersion in liquid nitrogen-cooled isopentane; transverse, 10- $\mu$ m-thick sections were cut with a Leica cryostat and placed onto Superfrost Plus slides (Fisher Scientific Co.). Slides were stored at −20 or −80°C until use. For

use, slides were returned to room temperature, immersed briefly in acetone at −20°C, washed in PBS (137 mM NaCl, 2.68 mM KCl, 10 mM Na<sub>2</sub>HPO<sub>4</sub>, and 1.76 mM KH<sub>2</sub>PO<sub>4</sub>, pH 7.4), and incubated in primary antibody for 2 h at room temperature or overnight at 4°C. Primary antibodies were diluted in PBS containing 2% goat serum, or 2% BSA, or both. Sections were washed in PBS containing 0.05% Tween 20 and incubated in species-appropriate, affinity-purified, fluorescently labeled secondary antibodies diluted in 2% goat serum in PBS for 1 h at room temperature. After washes in PBS-Tween 20, stained slides were mounted in fluoromount-G (Southern Biotechnology Associates, Inc.) or in Prolong (Molecular Probes, Inc.) to reduce photobleaching.

In situ hybridization was performed as previously described (Libby et al., 1997) using cRNA probes generated from mouse  $\beta$ -netrin cDNAs, a mouse netrin-1 cDNA (isolated in our laboratory by PCR), and a mouse *wnt-1* cDNA (obtained from B. Morgan, Harvard University, Cambridge, MA). cDNA templates were synthesized by PCR (mouse E17 cDNA). The reverse primer T7 polymerase recognition site sequence (TCCTACGACTCACTATAGGGAGG) was added to the 3' end of the following probes: for mouse netrin-1 (U65418), probe 1, nucleotides 267–764, and probe 2, nucleotides 1,213–1,708; for mouse  $\beta$ -netrin (AF281278) probe 1, nucleotides 340–826, probe 2, nucleotides 1,060–1,509, and probe 3, nucleotides 1,406–2,041. Slides were examined and photographed with a Spot digital camera (Diagnostic Instruments). Images shown here were created using Adobe Photoshop (Releases 4.0–5.5); no enhancements other than contrast and brightness have been made to these images.

### In Vitro Olfactory Bulb Neurite Outgrowth Assays

Timed pregnant Sprague-Dawley rats were killed according to protocols approved by institutional animal care committees. E15 embryos were collected and olfactory bulbs were removed into culture medium (DME [Bio-Whittaker] containing 10% FBS [Hyclone Laboratories Inc.], 100 U/ml penicillin, and 100  $\mu$ g/ml streptomycin [both from Irvine Scientific]) essentially as described elsewhere (Pini, 1993; Li et al., 1999). Olfactory bulbs were divided into three to six explants. At least two, but not more than four, explants were placed in a drop of 2.4 mg/ml collagen (Vitrogen; Cohesion Technologies), and the collagen drops were placed in a humidified 37°C incubator (5% CO<sub>2</sub>) for 45 min to gel. 500  $\mu$ l of culture medium or culture medium containing laminin or  $\beta$ -netrin proteins was added to each collagen drop. Explants were cultured at 37°C for 16–24 h and fixed in 4% paraformaldehyde (Polysciences) in PBS for 5 min at ambient temperature and processed for immunohistochemistry as previously described (Murrell and Hunter, 1999), using an antiserum against neural cell adhesion molecule (Chemicon International, Inc.), and a rhodamine-conjugated secondary antibody (Sigma-Aldrich) diluted in PBS containing 2% BSA (Sigma-Aldrich), and 0.01% Triton X-100 (Sigma-Aldrich).

Each explant was photographed digitally in multiple fields; the images were combined to create a composite containing the entire explant and all neurites. Neurite number and length, explant circumference and explant area were quantified by tracing from the composites using Scion Image (Release Beta 3b; Scion Corporation). Measurements for explants within each collagen gel were averaged, normalized to the control values for a particular culture, and plotted using Microsoft Excel 97 SR-2. Data are displayed as the percent control  $\pm$  SEM. The statistical significance of differences between any two conditions was analyzed using the *t* test; probability values of < 0.05 were judged significant.

### Other Methods

SDS-PAGE (Laemmli, 1970) and electrophoretic transfer of proteins to nitrocellulose with immunoblot analysis were performed essentially as described elsewhere (Lunstrum, et al., 1986). For chemiluminescence, primary as well as secondary antibodies (Amersham Life Science) were diluted 1:4,000 in 3% milk powder, PBS, and 0.5% Tween 20. For detection, the Renaissance solution from NEN Life Science Products was used according to the manufacturer's instructions. For the FISH analysis, a 1.7-kbp PCR product (nucleotides 1,114–2,946) was used for the fluorescent in situ localization of the  $\beta$ -netrin gene (SeeDNA Biotech, Inc.)

### Results

A novel partial cDNA sequence was identified in the dbEST sequence database by searching for sequences containing laminin EGF-like repeats. A 344-bp sequence was obtained and this sequence was extended using rapid am-

## Amino acid sequence of human and mouse $\beta$ -netrin

		50
domain VI	h	MGSQCARLLLL WGQTVVAAGL SGVAGVSSRC EKAQNPRMGN LALGRKLWAD
	m	---SA--- N---AN---R---
		100
h	TTCGQNA TEL YCFYSENKDL TCRQPKCDKC NAAYPHLAHL PSAMADSSFR	
m	-M----- F-----A-----HS-----P-----	
		150
h	FPRTWQSAE DVHREKIQLD LEAEFYFTHL IVMFKSPRPA AMVLDRSQDF	
m	-----M-----	
		200
h	GKTWKPKYKF ATNCSATFGL EDDVVKGAI CTSKYSSPFP CTGGEVIFKA	
m	-----R-----N-----	
		250
h	LSPPHDTENP YSAKVQEQLK ITNLRVQLLK RQSPCPQRND LNEEPQHFTH	
m	---Y-I---R-----I---AK-H---H	
		261
h	YAIYDFIVKG S	
m	--V-----	
		300
domain V	h	CFQNGHADQ QIPVHGFRPV KAPGTFHMVH GKCMCKHNTA
	m	---L--E---I---A--V---R---
		350
h	GSHQHQCAPL YNDRPWEAAD GKTGAPNECR ACKCNHGADT CHFVDVNWAEA	
m	-----R-----T-----	
		400
h	SGNRSGGVCD DCQHNTGQY CQRCKPGFYR DLRRPFSAPD ACKPCSCHPV	
m	-----N N-----H-----A-----	
		450
h	GSAVLPA NSV TFCDPNSNGDC PCKPGVAGR CDRCMVGYWG FGDYCGRCPCD	
m	---I--FS---PH-----	
		462
h	CAGSCDPITG DC	
m	-----L---	
		500
C domain	h	ISSHTDID WCHEVPDFRP VHNKSEPAWE WEDAQGFSA L
	m	---NA-V- -Y---T-HS M-----S---E---
		550
h	LHSGKCECKE QTLGNAKAFQ GMKYSYVLKI KILSAHDGRT HVEVNVKIKK	
m	R-----P-----S-----A-----	
		600
h	VLKSTLKIIF RGKRTLYPES WTRDRCQTCPI LNPGLLEYLVA GHEDIRTGKL	
m	-----L-----N-----V-----	
		628
h	IVNMKSFVQH WKPSLGRKVM DILKRECK	
m	-----A--R-- H---D-V	

**Figure 1.** Comparison of the predicted full-length amino acid sequences of human (h) and mouse (m)  $\beta$ -netrin. Amino acids in the human sequence that are conserved in mouse are indicated by dashes. A 19-amino acid signal sequence precedes the  $\beta$ -netrin NH<sub>2</sub> terminus; an arrowhead marks the signal peptide cleavage site. The predicted amino acid sequence of  $\beta$ -netrin contains three domains (large boxes): an NH<sub>2</sub>-terminal domain with homology to domain VI of laminin  $\beta$  chains, a domain with homology to the V domain of laminin  $\beta$  chains, and a COOH-terminal domain with homology to the C domain of netrins. Potential glycosylation sites are doubly underlined; all are conserved between human and mouse. EMBL/Genbank/DBJ accession numbers for the sequences reported here are as follows: mouse  $\beta$ -netrin, AF281278; human  $\beta$ -netrin, AF278532.

plification of cDNA ends, resulting in the full-length human cDNA. The mouse cDNA was obtained using nested PCR with human primers at low annealing temperature, and a nearly full-length sequence (lacking most of the 3'-UTR) was obtained. The cDNA contains a predicted open reading frame of 629 amino acids, including a 19-amino acid-long putative signal peptide that closely meets the criteria described by Nielsen et al. (1997) (Fig. 1). The predicted protein is a putative secreted molecule with an NH<sub>2</sub>-terminal domain similar to domain VI of the laminin  $\beta$  chains, which is a central domain containing EGF-like repeats similar to domain V of the laminin  $\beta$  chains, and a COOH-terminal domain homologous to the netrin C domains. The predicted human and mouse amino acid sequences contain 90% identical laminin VI domains, 91% identical laminin V

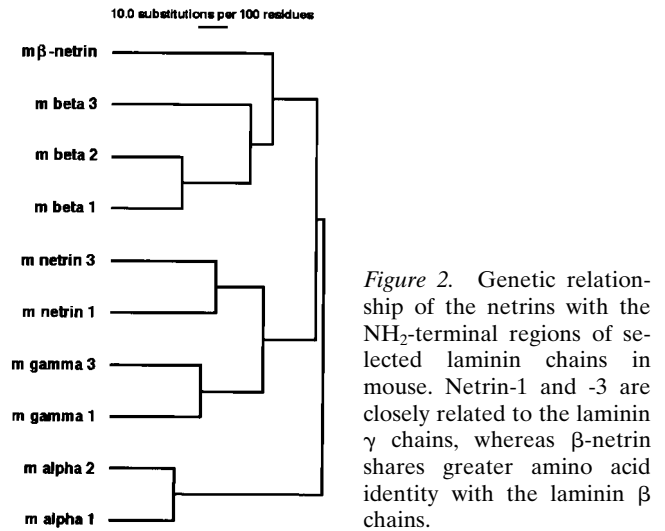


**Figure 2.** Genetic relationship of the netrins with the NH<sub>2</sub>-terminal regions of selected laminin chains in mouse. Netrin-1 and -3 are closely related to the laminin  $\gamma$  chains, whereas  $\beta$ -netrin shares greater amino acid identity with the laminin  $\beta$  chains.

domains, and 86% identical C domains. There are two consensus glycosylation sites: one in the VI domain and one in the C domain; both are present in mouse and human.

Thus, the overall structure of this novel molecule is similar to the family known as netrins. Three vertebrate netrins (netrins 1–3) have been described in the literature (see Introduction). All contain domains with homology to the laminin  $\gamma$  chain domains V and VI and a COOH-terminal domain.

The  $\beta$ -netrin V and VI domains are 43% identical to the laminin  $\beta$ 1 chain V and VI domains, 42% identical to those in the laminin  $\beta$ 2 chain, and 38% identical to those in the laminin  $\beta$ 3 chain (Fig. 2). The V and VI domains of  $\beta$ -netrin are 32% identical to those in the laminin  $\gamma$ 1 chain; for comparison, netrin-1 has 50% identity with the laminin  $\gamma$ 1 chain. Full-length mouse  $\beta$ -netrin is 31% identical to mouse netrin-1 and 28% identical to mouse netrin 3. Among all the netrins, the second EGF-like repeat is the most highly conserved ( $\beta$ -netrin versus netrin-1, 54% amino acid identity;  $\beta$ -netrin versus netrin 3, 56% identity); the EGF-like repeats 1 and 3 ranged from 26 to 39% amino acid identity.

### Recombinant Expression of $\beta$ -netrin

Full-length recombinant mouse  $\beta$ -netrin (r $\beta$ -N) including a His tag and thrombin cleavage site (r $\beta$ -N + His) was expressed using a mammalian expression vector in 293-EBNA cells. A shortened form of  $\beta$ -netrin lacking the C domain (r $\beta$ -N $\Delta$ C), and full-length recombinant mouse netrin-1 (rN1) were similarly produced. The expressed products were purified using a Ni-containing column, and the His tag was removed in some cases by thrombin cleavage.

Visualization of r $\beta$ -N by transmission electron microscopy after rotary shadowing indicates that the recombinant molecule is folded into structures resembling images of portions of laminin short arms. The globular VI domain at the NH<sub>2</sub> terminus measures  $\sim$ 8 nm in diameter and the short rod contributed by the EGF-like repeats and the C domain measures  $\sim$ 8.6 nm, giving an overall length of  $\sim$ 17 nm. Unexpectedly, the best interpretation of 44% of the images is that the molecules can associate to form dimers, and, to a lesser extent (1.5%;  $n = 788$ ), higher order assemblies (Fig. 3 A; a single representative field is shown; a portion of the field is shown at higher magnification in Fig. 3 B). The overall length of the dimer averages 24.6 nm, of

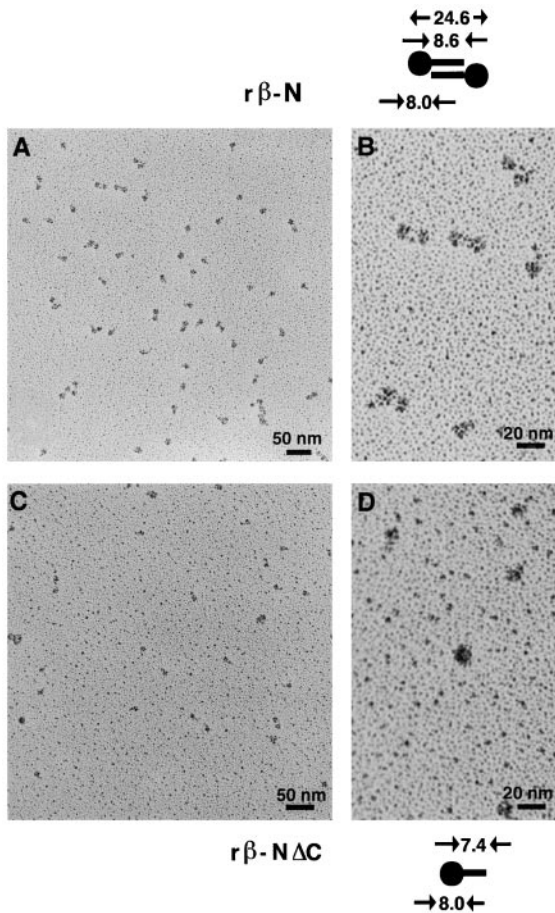


**Figure 3.** Transmission electron microscopic images of  $r\beta$ -N and  $r\beta$ -N $\Delta$ C obtained following rotary shadowing. Representative fields are shown. 44% of the images of full-length  $\beta$ -netrin (A and B) appear as dimers, whereas most of those of  $\beta$ -netrin lacking the C domain ( $r\beta$ -N $\Delta$ C) appear as monomers (C and D). The dimers appear to associate through an interaction of the V and C domains. The measured average sizes of the images of the dimers are shown in the models adjacent to B and D ( $n = 30$  monomers; 30 dimers).

which the two VI domains contribute 16 nm, leaving the VI domains separated by  $\sim 8.6$  nm. Therefore, the images are consistent with dimerization occurring through antiparallel linear alignment of the V and C domains (cartoons of the proposed structures are illustrated next to Fig. 3, B and D). On the other hand, in rotary shadowed preparations of  $r\beta$ -N $\Delta$ C, most molecules appear to be monomeric globules with a short rodlike projection (Fig. 3 C, a single representative field is shown; a portion of the field is shown at a higher magnification in Fig. 3 D); the only other form observed in preparations of the  $r\beta$ -N $\Delta$ C are multimeric aggregates, which we interpret as artefacts of the preparation.

The calculated mass of  $r\beta$ -N + His is 68 kD; it migrates with an electrophoretic mobility predicting a final mass of 70 kD (Fig. 4 A).  $r\beta$ -N $\Delta$ C + His has an electrophoretic mobility consistent with a mass of 56 kD (Fig. 4 A), which corresponds well with a predicted mass of 53 kD. Removal of the His tag by thrombin cleavage reduces the apparent molecular mass slightly, as expected.  $r\beta$ -N + His and  $r\beta$ -N $\Delta$ C + His, as well as recombinant laminin  $\beta$ 2 short arm containing a His tag are all recognized by an anti-His anti-

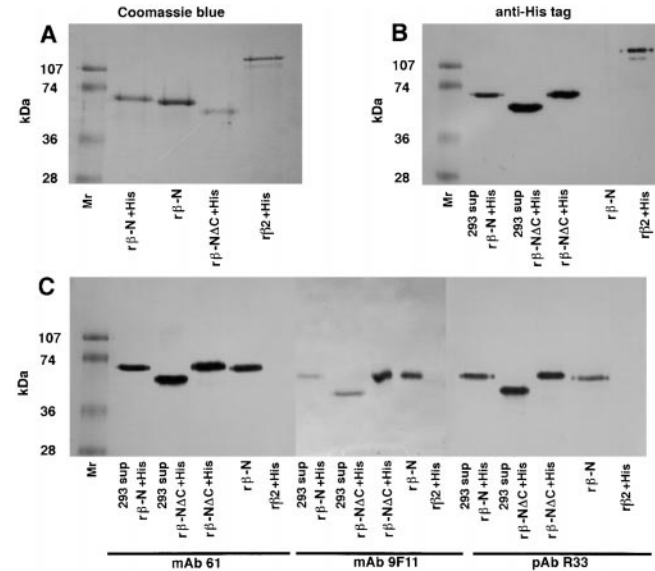


**Figure 4.** Electrophoretic profiles of  $\beta$ -netrin expression products and Western analysis using antibodies mAb61, mAb9F11, and pAbR33. (A) Comparison of the electrophoretic mobilities of purified full-length recombinant mouse  $\beta$ -netrin including the His tag ( $r\beta$ -N+His), full-length  $\beta$ -netrin with the His tag removed ( $r\beta$ -N), truncated  $\beta$ -netrin including the His tag ( $r\beta$ -N $\Delta$ C+His), and recombinant human laminin  $\beta$ 2 chain domains III–VI including the His tag ( $r\beta$ 2 +His).  $M_r$ , relative molecular mass standards. Proteins were visualized with Coomassie brilliant blue R-250. (B) Western blots of recombinant proteins using an anti-His antibody. Aliquots of culture media from 293-EBNA cells expressing full-length or truncated  $\beta$ -netrin were electrophoretically separated and His-containing proteins were detected using an anti-His antibody. Despite the fact that the netrins are minor components of the applied media, only single bands were detected in the positions expected for full-length or truncated  $\beta$ -netrin. Purified full-length  $\beta$ -netrin is detected only before removal of the His tag, indicating that this tag is fully eliminated by cleavage. Purified recombinant laminin  $\beta$ 2 chain short arm is present at sufficient concentration to be easily detected by Western blot. The nomenclature for the individual recombinant proteins is as in A. (C) Characterization of anti- $\beta$ -netrin antibodies by Western analysis of recombinant proteins. Three membrane blots identical to that described in B were probed with the antibodies mAb61, mAb9F11, and pAbR33. The patterns obtained using all three antibodies is identical: all recognize both the full-length and truncated forms of  $\beta$ -netrin, indicating that the epitopes recognized by the mAbs are within domains V or VI, and the polyclonal antiserum also recognizes epitopes within the same domain. None of the antibodies cross-reacts with the laminin  $\beta$ 2 chain short arm, nor with its His tag. The nomenclature for the individual recombinant proteins is as in A.

body, but there is no residual activity against  $r\beta$ -N after removal of the His tag (Fig. 4 B).

### **Production and Characterization of Polyclonal and Monoclonal Antibodies to $\beta$ -Netrin**

Rabbits and mice were immunized with  $r\beta$ -N + His. The rabbit antiserum was purified using protein G to obtain IgG, and the isolated antibodies were affinity-purified by column affinity chromatography using CNBr-activated Sepharose with attached  $r\beta$ -N $\Delta$ C, from which the His tag had been removed by thrombin cleavage. The product of this protocol is

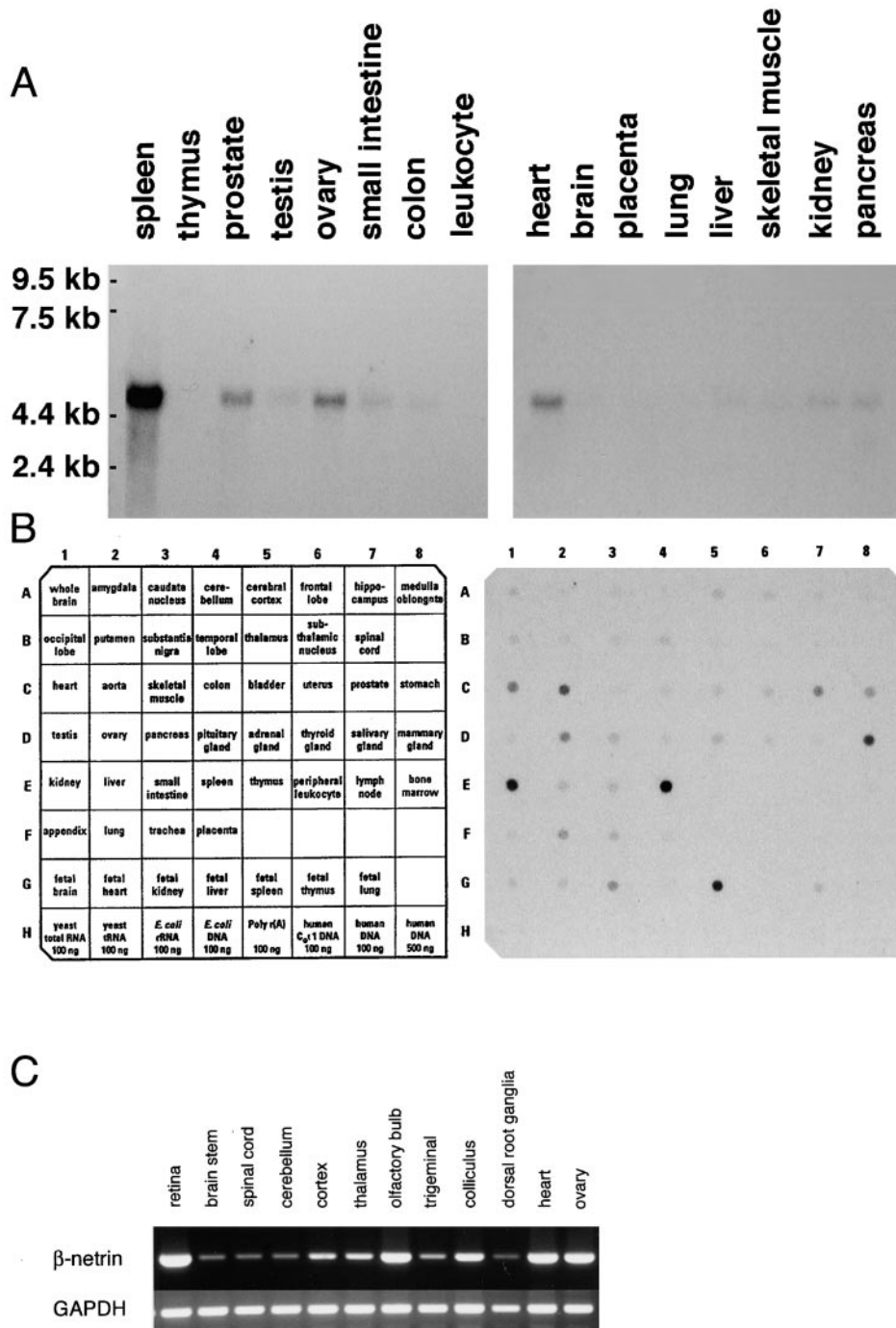


**Figure 5.**  $\beta$ -Netrin RNA is expressed widely in human and mouse tissues. The same cDNA probe was used to probe adult human tissue blots (A) and a dot blot (B). Only a single major RNA species is detected on the tissue blots. Strong signals are present in spleen, prostate, ovary, heart, kidney and pancreas, mammary gland, and uterus. Only weak signals are present in brain tissue. (C) RT-PCR confirms strong expression of  $\beta$ -netrin RNA in adult mouse kidney, heart, and ovary, as expected from the human blot analyses. In addition,  $\beta$ -netrin RNA is readily detected in several CNS structures including, olfactory bulb and retina. Some expression is observed in other brain regions; however, spinal cord, brain stem, and dorsal root ganglia contain only low levels of  $\beta$ -netrin RNA.

termed pAbR33. Hybridomas were produced from mouse splenic lymphocytes, and clones 9F11 and 61 were determined to react with r $\beta$ -N and with r $\beta$ -N $\Delta$ C by ELISA (data not shown) and by Western blot analysis.

All three antibody preparations, pAbR33, mAb9F11, and mAb61, react identically by Western blot analysis. Specifically, all three react with a single band in the supernatants from cultured 293-EBNA cells expressing either r $\beta$ -N + His or r $\beta$ -N $\Delta$ C + His. Coomassie blue staining of these culture supernatants shows multiple bands with the same or greater intensity than seen for the expression product (not shown). The identified bands have electrophoretic mobilities identical to r $\beta$ -N + His or r $\beta$ -N $\Delta$ C +

His (Fig. 4 C). Removal of the His tag has no effect upon the antibodies ability to recognize either recombinant protein (Fig. 4 C). Thus, all three antibody preparations clearly recognize epitopes in domains V and VI of the molecule. None of the antibodies reacts with the recombinant laminin  $\beta$ 2 short arm, which includes the His tag, by Western analysis (Fig. 4 C).

Given the high amino acid identity among the laminins and in the netrins in the V and VI domains, we compared the reactivity of our antibody preparations to known expression patterns of laminin chains. Although all of the antibodies are useful in immunohistochemistry (see below), none reacts with the basement membrane at the dermal-

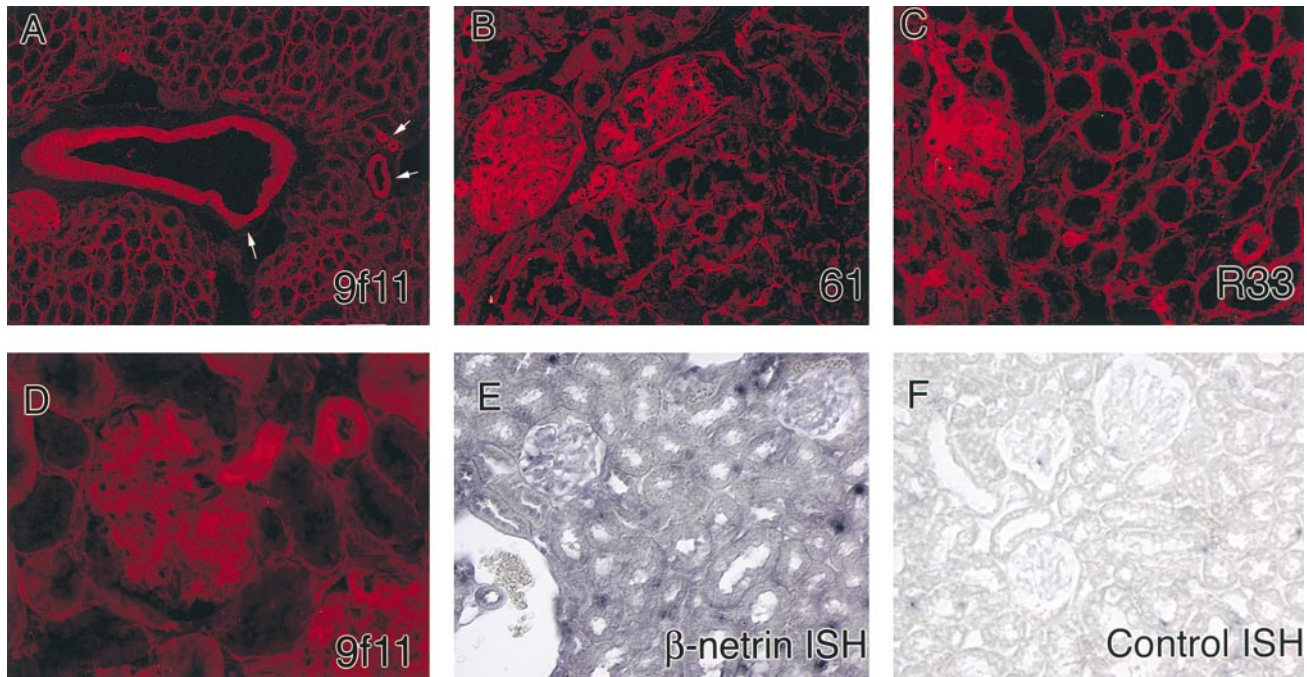


**Figure 6.**  $\beta$ -Netrin is expressed and deposited in basement membranes throughout the adult rat kidney.  $\beta$ -Netrin was detected by indirect immunofluorescence using three different anti- $\beta$ -netrin antibodies (indicated).  $\beta$ -Netrin immunoreactivity can be observed within the major and minor arteries (arrows in A), and in the afferent arterioles (B–D). All portions of the tubules are recognized by the antibodies (A–C), as is the mesangium of the glomeruli (B–D). In situ localization of  $\beta$ -netrin RNA shows reaction product deposited throughout the kidney (D; control probe shown in E), consistent with the protein localization. Bars: (A) 100  $\mu$ m; (B, C, E and F) 50  $\mu$ m; (D) 25  $\mu$ m.

epidermal junction of skin by immunohistochemistry (data not shown). Therefore, none of these antibodies cross-reacts with the laminin  $\beta$ 1,  $\beta$ 3,  $\gamma$ 1, or  $\gamma$ 2 chains. The distribution of  $\beta$ -netrin in the retina is also different than the distribution of either the laminin  $\beta$ 2 or  $\gamma$ 3 chain (data not shown); therefore, we conclude our antibodies are not cross-reacting with these laminin chains.

The monoclonal anti-r $\beta$ -N antibody, 9F11, recognizes a conformation-specific epitope. No reactivity of 9F11 is observed after the disulfide bond reduction of the electrophoretic sample (data not shown). The  $\beta$ -netrin species identified by 9F11 in Fig. 4 C was not reduced, whereas those identified with the monoclonal 61 or pAbR33 were disulfide bond-reduced products. The species identified by all the antibodies in Fig. 4 C have the same electrophoretic mobilities, indicating that the molecules are not associated into disulfide-bonded aggregates. These data indicate that the  $\beta$ -netrin dimers visualized by rotary shadowing are not stabilized covalently.

#### **Tissue Distribution of $\beta$ -Netrin RNA**

RNA expression analysis (Fig. 5, A and B) of  $\beta$ -netrin in human tissues showed that  $\beta$ -netrin is most highly expressed in kidney, spleen, mammary gland, aorta, heart, ovary, prostate, and fetal spleen. Next, we performed semi-quantitative RT-PCR on various mouse tissues and confirmed that, as in humans,  $\beta$ -netrin expression is high in kidneys, hearts, and ovaries (Fig. 5 C). However, we obtained signals from neural tissues as well (Fig. 5 C). A strong signal was obtained from the whole brain (not shown) and retina; fractionation of the whole brain into component regions

(Fig. 5 C) demonstrates a low level of expression in most regions, with the exception of the olfactory bulb, where the signal strength approached those obtained from the kidney, heart, and ovary. Below, we have focused our histological studies on those tissues in which PCR signals were high; our studies of the retina will be reported elsewhere.

#### **Comparison of the Tissue Distribution of $\beta$ -Netrin RNA and $\beta$ -Netrin Protein**

Tissue distribution of the  $\beta$ -netrin protein was determined by indirect immunofluorescence in various rat tissues and the cellular sources of  $\beta$ -netrin were determined by in situ hybridization. One immediately obvious generalization is that  $\beta$ -netrin is expressed in the basement membranes of a variety of tissues (see Figs. 6–9). In the kidney (Fig. 6),  $\beta$ -netrin protein is expressed in the basement membranes of all tubules. The major arteries and arterioles (Fig. 6 A, arrows) were prominently reactive; also strongly reactive were the afferent arterioles (Fig. 6, C and D). Particularly clear was the reactivity in the basal lamina surrounding the smooth muscle cells in the wall of the vessels. In addition,  $\beta$ -netrin immunoreactivity was present in the basement membrane of the rat glomerulus. This pattern of immunoreactivity is different than that reported for the laminin  $\beta$ 2 chain (Hunter et al., 1989), further supporting a lack of cross-reactivity between these molecules.  $\beta$ -Netrin transcripts, as judged by in situ hybridization, are localized to all cells in the kidney (Fig. 6 E), including the tubular epithelial, vascular endothelial, mesangial, and Bowman's capsule cells; an equally well labeled probe with a similar G-C content showed no hybridization (Fig. 6 F). These ob-

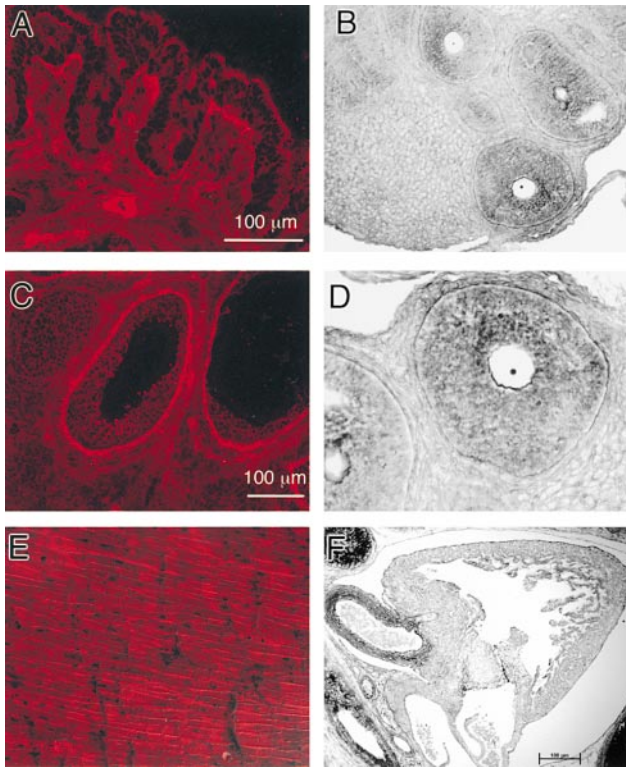


**Figure 7.**  $\beta$ -Netrin is expressed and deposited in the basement membranes of the adult rat fallopian tube and ovary. (A) R33 antiserum shows  $\beta$ -netrin deposition in the basement membranes underlying the fallopian epithelium, and the arterial smooth muscle in the underlying lamina propria. Some reactivity also appears at the epithelial apical surface. (B) In situ hybridization in the ovary demonstrating that secondary follicles have a high level of expression of  $\beta$ -netrin transcripts. Surrounding primary follicles are less well labeled. The scale here is twice C. (C)  $\beta$ -Netrin is expressed and deposited in the basement membranes of the adult rat ovary. With the R33 antiserum, a strong signal is observed in the basement membrane of the secondary follicles, as well as surrounding arterial smooth muscle. The marker is 100  $\mu$ m. (D) Higher power view of the in situ hybridization in maturing follicles; high levels of expression of  $\beta$ -netrin transcripts are observed in the perifollicular cells. Primary follicles, which surround the maturing ones, are less well labeled. The scale is as in B. (E)  $\beta$ -netrin immunoreactivity in the adult heart. Immunoreactivity is concentrated in the interstitial spaces surrounding cardiac myocytes. The scale is one quarter that of F. (F) In situ hybridization in fetal heart shows prominent labeling in the ventricular muscle wall as well as very high levels of expression in the smooth muscle of the aorta and pulmonary vessels. Bar, 100  $\mu$ m (in F).

servations suggest that  $\beta$ -netrin is a prominent element of the basement membrane and that both the epithelium and the mesenchyme contribute to its production.

As the RNA expression (Fig. 5) suggested high levels of  $\beta$ -netrin expression in the ovary, we examined the distribution of  $\beta$ -netrin in the female reproductive system. Tissue distribution of  $\beta$ -netrin in the ovary and the fallopian tube showed analogous distribution. For example,  $\beta$ -netrin immunoreactivity was a prominent element of the basement membrane of the fallopian tube (Fig. 7 A) and the arterial smooth muscle in the lamina propria (Fig. 7 A). In addition to the basal reactivity, there is some  $\beta$ -netrin immunoreactivity at the apical surface of the epithelium, sug-

gesting the fallopian epithelium is at least one source of the molecule. In situ hybridization confirms this suggestion, and demonstrates that  $\beta$ -netrin transcripts are localized to the apical and basal ends of the fallopian epithelium (data not shown).

The ovary expresses  $\beta$ -netrin as well; in this tissue, in contrast to both the kidney and the fallopian tube, there is a developmentally regulated appearance of  $\beta$ -netrin. Specifically,  $\beta$ -netrin immunoreactivity is observed only in the basement membrane of the secondary or mature follicles (Fig. 7 C); primary follicles are not reactive (Fig. 7, B and D). Dense alkaline phosphatase reaction product localizing RNA transcripts for  $\beta$ -netrin are observed in the large maturing follicles, whereas the primary follicles are more lightly labeled (Fig. 7 B). Control sections with a similarly well-labeled probe do not label the ovary (data not shown).

Immunoreactivity was also present in the perimysium of the heart (Fig. 7 E), where  $\beta$ -netrin is expressed surrounding individual muscle cells; in situ hybridization localizes transcripts to the cardiac wall and the aorta during embryonic development, E15.5 (Fig. 7 F). We also examined the spleen; our analysis was complicated by high background binding of secondary antibodies to splenocytes, but  $\beta$ -netrin is prominently expressed in this tissue (not shown, but see RNA expression in Fig. 5). There appeared to be more reactivity in red pulp than in white.

As netrin-1 and netrin-2 are classically described as neural guidance molecules produced by the floorplate; we investigated whether  $\beta$ -netrin was expressed in the developing spinal cord along with netrins 1 and 2. We looked at E11.5 to E17.5 mouse embryos and found only diffuse immunoreactivity, which we could not distinguish from control sections (data not shown). Next, we turned to in situ hybridization using tissue from E11.5, E15, and E17 embryos. We compared the  $\beta$ -netrin expression pattern to that of the two other developmentally regulated molecules, netrin-1, which is expressed by the floorplate, and *wnt1*, which is expressed by the roofplate. In situ hybridizations confirm the expression of both of these molecules at E11.5. Netrin-1 is expressed at high levels in the floorplate (Fig. 8 A); expression levels are above background in the ventricular epithelium to the midpoint of the dorsal-ventral axis. Expression of *wnt1*, on the other hand, is confined to a small number of cells in the roofplate (Fig. 8 B). None of the three cRNA probes (generated to different regions of the  $\beta$ -netrin RNA) showed convincing levels of expression in the cord or in the dorsal root ganglion (two probes are shown in Fig. 8, C and D) at this age or earlier ages.

We also examined the adult brain, focusing on the area in which our RT-PCR results suggested there was high expression. In contrast to the brilliant staining of peripheral basement membranes,  $\beta$ -netrin expression in the brain was more difficult to interpret until we focused on selected regions of the brain in which RT-PCR showed high levels of expression. For example, in the olfactory bulb, we observed a clear expression pattern. In situ hybridization confirmed the presence of  $\beta$ -netrin transcripts within the olfactory bulb (Fig. 9 A); specifically, in the periglomerular cells and the lateral olfactory tract; in addition, the ventricular epithelium showed considerable binding of the  $\beta$ -netrin antisense probes and some expression was detected in the mitral cell layer. Immunohistochemistry demonstrated  $\beta$ -netrin immunoreactivity within the lateral ol-



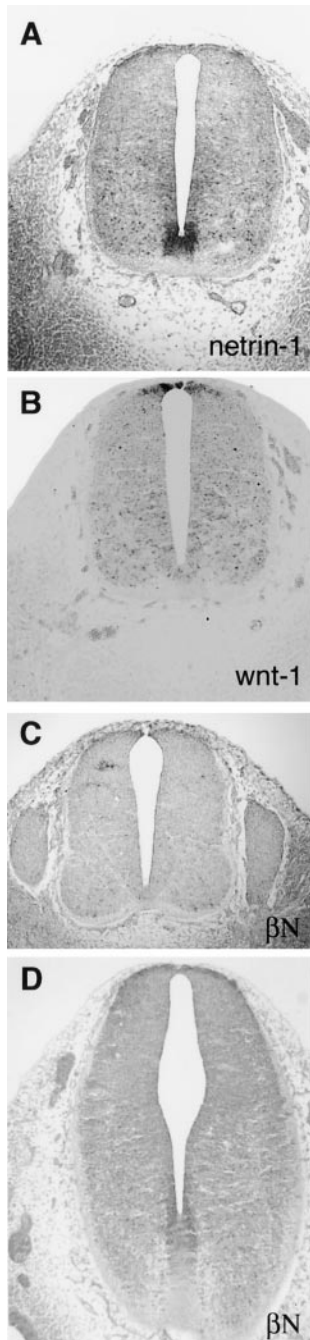


**Figure 8.**  $\beta$ -Netrin RNA appears not to be expressed in the floorplate of midgestation mouse embryos. (A and B) nonradioactive in situ hybridizations of floor- and roof-plate markers (netrin-1, and wnt-1) show good localization of transcriptions to these structures, respectively. (C and D) Two different probes for  $\beta$ -netrin, on the other hand, fail to localize to any region in embryonic day 11.5 spinal cord; in D we see some above background reactivity in the lateral margins of the floorplate.

factory tract (Fig. 9 B) as well as in the perineurium of the vomeronasal nerve (Fig. 9 C); only a weak, diffuse immunoreactivity was observed in the glomeruli of the olfactory bulb. Finally, there was strong deposition of  $\beta$ -netrin immunoreactivity in the basement membranes of the vascular supply of the brain as well as in capillary beds (Fig. 9, B and C). We observed this reactivity throughout the brain. We also detected in situ hybridization signals in vascular endothelial cells and the choroid plexus at embryonic ages (E15.5; data not shown).

#### Effects of $\beta$ -Netrin on Neurite Outgrowth

Because of the similarity in structure of  $\beta$ -netrin to netrins 1–3, and because  $\beta$ -netrin expression was detected in the output pathways of the olfactory bulb and the retina, we

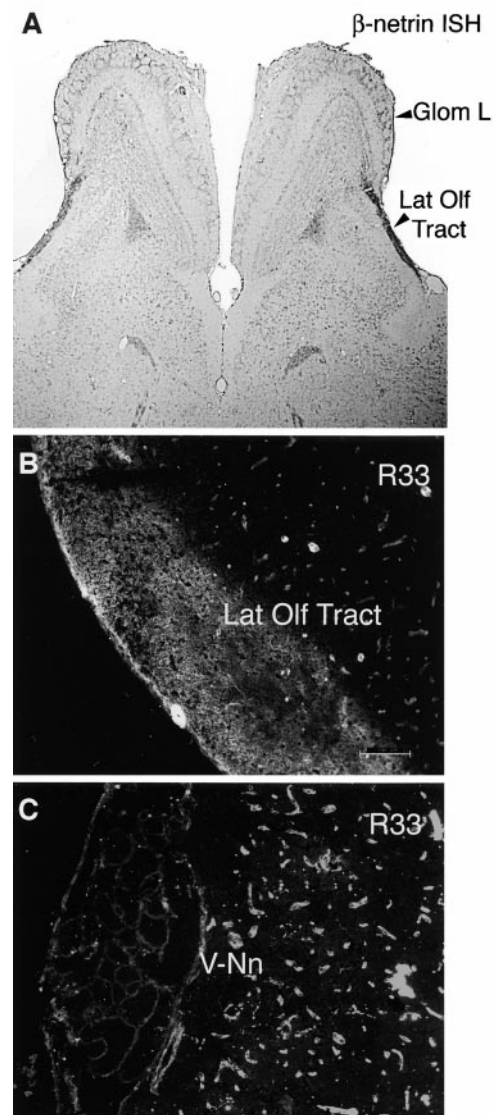


**Figure 9.**  $\beta$ -Netrin is expressed in the adult rat olfactory bulb. (A) Heavy in situ reaction product is observed over the lateral olfactory tract, the output pathway from the bulb (arrowhead, Lat Olf Tract); in the periglomerular cells (arrowhead, Glom L); and in mitral cell layer, the projection neurons of the bulb. Some reaction product is observed in the ventricles, ependyma and perhaps the blood vessel epithelium. (B and C) Protein localization by indirect immunofluorescence shows immunoreactivity in the lateral olfactory tract and the perineurium of the vomeronasal nerve (V-Nn). In addition, considerable immunoreactivity is observed in the basement membrane of the blood vessels.

tested the ability of  $\beta$ -netrin to promote neurite outgrowth. Explants of E15 rat olfactory bulb were dissected, embedded in collagen gels, and incubated with soluble recombinant full-length and truncated  $\beta$ -netrin ( $r\beta$ -N and  $r\beta$ - $\Delta$ NC; Fig. 10). In control cultures, neurites extend around the circumference of the explant (Fig. 10 A). Treatment with  $r\beta$ -netrin increases both the neurite length and the number of neurites extending from cultures (Fig. 10, B and C). We measured several parameters of this increase in neurite outgrowth including the following: total number of neurites; average neurite length; total length of

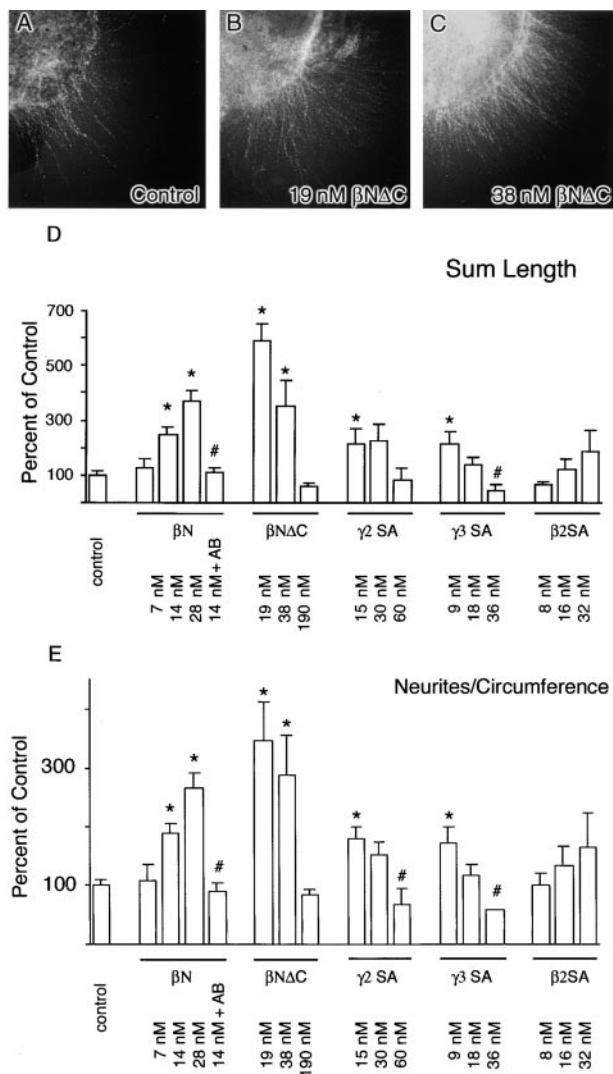


**Figure 10.**  $\beta$ -Netrin produces neurite outgrowth from olfactory bulb explants. (A–C) Representative cultures treated as indicated. Treatment with  $r\beta N\Delta C$  or full-length  $r\beta N$  proteins increases the number of neurites produced by the explants. (D) Quantification of data obtained on neurite outgrowth; the total length of all neurites produced by explants is given here (Sum Length). Protein additions are noted below the bars; the line indicates that cultures were treated identically; the concentrations of protein additions are noted below the line.  $\beta$ -Netrin conventions are as above; 14 nM + AB indicates the simultaneous addition of 14 nM  $\beta N$  and pooled polyclonal antisera to  $\beta N$ .  $\gamma 2SA$  denotes the short arm of the laminin  $\gamma 2$  chain; similar conventions are used for  $\gamma 3$  and  $\beta 2$  chains. \* Statistically significant difference versus control; # statistically significant difference versus 14 nM  $\beta N$  or 9 nM  $\gamma 3SA$ , respectively;  $P < 0.05$ .

neurites (sum neurite length); and total neurite area (Table I). By all measures, the addition of  $r\beta$ -N produced an increase in neurite outgrowth; these data are shown graphically in Fig. 10. With the addition of  $r\beta$ -N, there was a dose-dependent increase in both the sum length of all neurites and the number of neurites (normalized to explant circumference) of up to 400% of control measurements (Fig. 10, D and E,  $r\beta$ -N); values in the presence of all but the lowest concentration of  $r\beta$ -N were statistically different from control values ( $P < 0.05$ ). The addition of an affinity-purified preparation of pooled anti- $\beta$ -netrin anti-

sera antagonized this effect, reducing neurite length and number to control levels.

The addition of the truncated version of  $\beta$ -netrin missing the C domain,  $r\beta$ -N $\Delta C$ , to explants also increased the total neurite length and the number of neurites extending from the explants (Fig. 10, D and E,  $\beta$ -N $\Delta C$ ). However, with increased concentrations of the truncated form of the molecule, the neurite length and number returned to control levels; biphasic responses to netrin application are well documented in the literature (Serafini et al., 1994). We also tested the effect of homologous regions of laminin chains on this system: we tested expressed short arm fragments of both laminin  $\gamma 2$  and  $\gamma 3$  chains as well as similar fragments of the laminin  $\beta 2$  chain. The addition of recombinant fragments of the laminin  $\gamma 2$  or  $\gamma 3$  chains increased neurite extension, measured either as sum length or number of neurites (Fig. 10, D and E,  $\gamma 2$  SA and  $\gamma 3$  SA) but both  $\gamma$  chain short arms were slightly less effective at stimulating outgrowth than  $\beta$ -netrin. Interestingly, increasing the dose of the added laminin  $\gamma$  chain short arms had decreased efficacy on neurite stimulation, which is similar to that observed with  $r\beta$ -N $\Delta C$ . On the other hand, the short arm fragment of the laminin  $\beta 2$  chain had no statistically significant effect on neurite extension over the concentration range we tested (Fig. 10, D and E,  $\beta 2$  SA).

### Chromosomal Localization

Using FISH, the gene encoding  $\beta$ -netrin was localized to human chromosome 12, region q22-q23 (not shown). Near this site are several genes associated with human ovarian cancer.  $\beta$ -Netrin cDNA sequences have been identified in the dbEST databases derived from ovarian and cervical cancers, and multiple sclerosis.

### Discussion

#### The Netrins Are a Family of Laminin-like Molecules

The netrins now define a family of molecules related to the  $NH_2$  termini of laminin chains (Fig. 11). Netrins 1–3 all are more related to the laminin  $\gamma$  chain than they are to other laminin chains, whereas the molecule reported here,  $\beta$ -netrin, is structurally related to the laminin  $\beta$  chains. However, it must be noted that Unc-6 (netrin-1) retains hallmarks of both  $\beta$  and  $\gamma$  chain specifically in the second EGF repeat (Wadsworth et al., 1996), where there is considerable homology among the netrins and laminins (see above).

Given that there are three laminin chain isoforms ( $\alpha$ ,  $\beta$ , and  $\gamma$ ), there are likely to be additional members of the netrin family, as there have been no laminin  $\alpha$  chain netrin analogues reported as yet. Indeed, we have identified two additional netrinlike molecules (Fig. 11); one of these has a putative transmembrane domain. These molecules have laminin-like domains VI and V resembling the laminin short arm. However, these molecules do not have the C domain present in the known netrins and, thus, are likely to form a novel subfamily. The complete identification of these molecules will be reported elsewhere. However, their existence suggests that a large family of laminin short-arm-related molecules exist and that they are broadly distributed and may have diverse functions beyond the oft-studied axonal guidance properties of the netrins.

Table I. Outgrowth from Olfactory Bulb Explants

	No. of experiments	No. of explants	Percent of control				
			Sum neurite length	Average neurite length	Neurite area	Neurites per circumference	No. of neurites
Control	24	52	100 ± 14	100 ± 4	100 ± 10	100 ± 11	100 ± 11
rβ-netrin							
7 nM	6	11	127 ± 31	109 ± 7	143 ± 23	108 ± 28	131 ± 25
14 nM	20	41	246 ± 32*	139 ± 11*	160 ± 8*	188 ± 18*	189 ± 17*
28 nM	10	16	368 ± 39*	154 ± 10*	197 ± 25*	265 ± 26*	265 ± 17*
14 nM + Ab	6	12	108 ± 18‡	121 ± 15	112 ± 18‡	90 ± 15‡	100 ± 13‡
rβ-netrin ΔC							
19 nM	4	8	587 ± 63*	168 ± 11*	235 ± 18*	344 ± 68*	370 ± 48*
38 nM	4	8	355 ± 91*	135 ± 16	136 ± 26	285 ± 70*	279 ± 46*
190 nM	5	15	65 ± 10	85 ± 18	64 ± 18	84 ± 9	78 ± 11
ry2							
15 nM	10	20	217 ± 50*	113 ± 9	136 ± 25	178 ± 23*	185 ± 29*
30 nM	9	24	225 ± 60	130 ± 18	139 ± 26	151 ± 24	166 ± 27
60 nM	3	8	82 ± 48	106 ± 15	65 ± 31	68 ± 27‡	91 ± 53
ry3							
9 nM	10	23	215 ± 45*	122 ± 14	146 ± 26	172 ± 28*	177 ± 28*
18 nM	10	23	139 ± 27	102 ± 5	96 ± 13	117 ± 18	140 ± 24
36 nM	2	7	47 ± 19	150 ± 65	49 ± 31‡	58 ± 0‡	42 ± 32‡
rβ2							
8 nM	3	8	65 ± 14	70 ± 6*	51 ± 8*	99 ± 22	89 ± 19
16 nM	6	23	124 ± 12	103 ± 12	107 ± 26	132 ± 34	123 ± 31
32 nM	3	10	188 ± 77	128 ± 16‡	192 ± 81	164 ± 58	166 ± 43

\*P < 0.05 versus control.

‡P < 0.05 versus 7 nM rβ-netrin.

§P < 0.05 versus 15 nM ry2, 9 nM ry3, or 8 nM rβ2.

Structurally, β-netrin is similar in most respects to the other members of the netrin family. Our observation that β-netrin can form dimers, however, was unexpected, as such data has not been reported to our knowledge for the other members of the family. The rotary-shadowed images are most consistent with dimerization occurring via interactions in the C domain of one molecule with the V domain of its partner, as the VI domains are separated by the approximate length of one, but not two, V and C domains. If β-netrin dimerizes in vivo, this could have implications for signal transduction. For example, dimers could cluster β-netrin receptors on individual cells, or it could bridge two cells expressing β-netrin receptors. Indeed, the dimerization of netrin receptors is a critical feature of netrin signaling, as the heterodimerization of the Unc5h2 and DCC netrin receptors is necessary and sufficient to convert netrin attraction to repulsion (Hong et al., 1999); however, receptor dimerization occurs even with monomeric ligand (Hong et al., 1999). Some caution must be used until the biologically active sites are defined as dimerization may in fact reduce activity (see below) and the availability of effector binding sites.

Of the previously reported netrins, only two (netrins 1 and 3) have been identified in the mouse (Puschel, 1999; Wang et al., 1999); netrin-2 has not. Is β-netrin the mammalian equivalent of netrin-2? This is unlikely, as netrin-2, like netrins-1 and -3, is more closely related to the laminin γ chains, whereas β-netrin is a laminin β chain homologue. Moreover, the distribution of β-netrin is unlike that of the previously described netrins. Although much of the work on netrins 1 and 2 has focused on the role of these molecules in neural development, they are widely expressed outside the nervous system. This new member of the family is expressed primarily outside the nervous system, most

abundantly in the vasculature, kidney, ovary, and the heart. Netrin-3 is highly expressed in somatic tissues, particularly in the lungs and heart (Puschel, 1999; Wang et al., 1999). The function of the netrins outside the nervous system has not been well studied.

Within the nervous system, the expression of β-netrin is limited largely to the retina and olfactory bulb. In our hands, β-netrin is not expressed in the spinal cord or in the dorsal root ganglion, unlike netrins 1–3. Our in situ results and immunohistochemical localization failed to demonstrate any β-netrin in the floorplate or DRG during development and in adult tissue. β-Netrin is expressed within the CNS vasculature, both in large muscular arteries as well as small capillaries, and in the ventricular ependymal

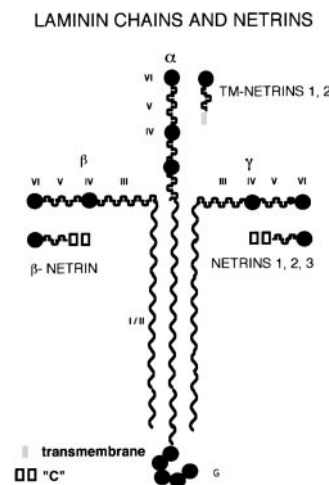


Figure 11. Cartoon of laminin and netrin families. Three classes of netrin molecules have been described; netrins 1–3 are more related to laminin γ chains, whereas the netrin reported here, β-netrin, is more related to the laminin β chains. Two additional molecules, one of which is a putative transmembrane molecule and are homologous to the short arm of laminin chains, have been found (see text for details; for simplicity they are shown along side the α chain). Thus, there is a growing family of molecules which have homology to the short arms of laminin molecules.

cells. Thus,  $\beta$ -netrin could have an important role in CNS angiogenesis; indeed, its expression outside the nervous system in somatic vasculature supports this suggestion.

### *$\beta$ -Netrin Is a Basement Membrane Molecule*

Unlike investigations of netrins-1 and -3, which have largely relied on RNA expression and predicted the protein localization from those data, we have produced three antibody preparations that reliably detect  $\beta$ -netrin on both blots and tissue sections and have demonstrated where  $\beta$ -netrin protein is deposited. Befitting its origin as a laminin-like molecule,  $\beta$ -netrin is deposited in the basement membranes of a variety of tissues, most prominently the kidney, ovary, heart and vasculature. While the location of a netrin in these regions may be surprising to some, it is not without precedent, as the localization of netrin-1 to the perimeter of the spinal cord in the region of the pia, a basement membrane-like structure in the CNS, has been reported in the chicken (MacLennan et al., 1997) and Unc-6 is considered part of the body wall basement membrane (Hedgecock et al., 1990; Wadsworth et al., 1996). These observations are seemingly at odds with the diffusible chemotropic hypothesis of netrin action. Specifically,  $\beta$ -netrin is deposited in close apposition to the source of synthesis. For example,  $\beta$ -netrin RNA is expressed in the tubules of the kidney and the epithelium of the fallopian tube;  $\beta$ -netrin protein is deposited in the subjacent basement membranes. In situ hybridization on large blood vessels shows that the  $\beta$ -netrin message is localized to the smooth muscle wall of the vessels, as is  $\beta$ -netrin protein (Figs. 6, 7, and 9). We have confirmed smooth muscle as one source of this molecule by isolating the protein from supernatants of primary cultures of smooth muscle cells (data not shown); however, we cannot exclude the endothelium as another source.

The colocalization of  $\beta$ -netrin RNA expression and protein deposition is less consistent with the chemoattractive or chemorepulsive mechanisms that have been suggested for the other netrins. Gradients of protein expression have been postulated for these molecules (Kennedy et al., 1994; Serafini et al., 1994). In the case of netrin-1 such a gradient may exist across the spinal cord, as there is a point source for netrin-1 in the floorplate and the netrin-1 protein appears to be localized to the perimeter of the spinal cord and the adjoining pial basement membrane. Thus, given a source (floorplate) and an apparent sink (in the pial basement membrane), there may be a gradient, the grade of which will be determined by the turnover of the molecule at both source and sink. In contrast, in the CNS,  $\beta$ -netrin RNA and  $\beta$ -netrin protein are present in immediately adjacent structures. For example, RNA transcripts are observed in the lateral olfactory tract and protein is deposited there. Thus, there does not appear to be the possibility of a gradient of  $\beta$ -netrin expression, unless it is a very steep one. However, caution should be used in interpreting these data, as a demonstration of developmental gradients of soluble signaling molecules is difficult and our antibodies may only detect the sinks for  $\beta$ -netrin where its concentration will be the highest.

Nonetheless,  $\beta$ -netrin may be important in axon guidance or pathfinding in the CNS. Disruptions of basement membranes, netrins, ECM elements, and their receptors

produce a wide variety of disruptions in axon guidance and neuronal migration (Przyborski et al., 1998; Deiner and Sretavan, 1999; Yee et al., 1999; Alcantara et al., 2000; Goldowitz et al., 2000; Walsh and Goffinet, 2000). These processes, although conceptually different, may differ formally only by the translocation, or lack thereof, of the cell body. One neuroactive component of the epidermal basement membrane in *C. elegans* is Unc-6 itself (Hedgecock et al., 1990; Ishii et al., 1992); indeed, HA-tagged Unc-6 molecules are secreted and incorporated into the matrix around secreting cells, seemingly assembling into the basement membrane (Wadsworth et al., 1996), suggesting that this basement membrane can act as a repository for neural guidance molecules. Other components of the basement membrane can also affect pathfinding; for example, mutations in *C. elegans* that disrupt the expression of the basement membrane component, nidogen, do not disrupt formation of the basement membrane per se but do produce defects in axonal migration (Kim and Wadsworth, 2000); specifically, axons that are normally laterally directed are redirected to the midline, and there are pathfinding defects in other identified axons as they cross the midline. Thus, the authors suggest that the body wall contains specialized subsets of basement membranes, which are important cues for guiding circumferential versus longitudinal migrations. Therefore, basement membrane components participate directly in determining the pathways of subsets of axons.  $\beta$ -Netrin may be another basement membrane component that provides such guidance cues. Functional disruptions of  $\beta$ -netrin using genetic systems or other approaches will resolve this speculation.

### *$\beta$ -Netrin Affects Neurite Outgrowth*

An initial step in defining the developmental role of  $\beta$ -netrin was taken in this study. The localization of  $\beta$ -netrin within the lateral olfactory tract, and the well-documented ability of netrins to direct neurite outgrowth, prompted us to determine if  $\beta$ -netrin supported neurite extension. Indeed, the addition of purified  $\beta$ -netrin to our culture system promoted neurite elongation. Specifically, the parameter most affected was apparently the initiation of elongation, which is the number of neurites produced, in contrast to any measure of length of neurites (Table I).

This finding suggests that  $\beta$ -netrin is a permissive signal and stimulates neurite elongation. Coupled with the expression data, it suggests that  $\beta$ -netrin acts by stabilizing the extending axons in some way. Since outgrowth frequently occurs by the overgrowth of pioneering axons by secondary axons, perhaps  $\beta$ -netrin is stabilizing the contacts between these jointly growing neurites, contributing to fasciculation. Indeed,  $\beta$ -netrin immunoreactivity is associated with the basal laminae in the perineurium of both the vomeronasal nerve (Fig. 9) and the optic nerve (data not shown). Alternatively, the incorporation of  $\beta$ -netrin into these basement membranes may contribute an inhibitory boundary function to these structures similar to what has been proposed for netrin-1, which is localized in the perimeter of the spinal cord (MacLennan et al., 1997). However, the stimulatory effect we see upon axon outgrowth from olfactory bulb explants argues against this possibility and suggests that  $\beta$ -netrin may be functioning in a fashion similar to netrin-1 which is expressed along

the optic pathway (Deiner and Sretavan, 1999) and disruptions of which disrupt ganglion cell routing (Deiner et al., 1997). However, it should be noted that netrins stimulate axonal elongation and cell migration in some systems and inhibit them in others (Serafini et al., 1994; Colamarino and Tessier-Lavigne, 1995; Wadsworth et al., 1996; Kim et al., 1999; Alcantara et al., 2000). Thus, the apparent stimulatory effect of  $\beta$ -netrin on olfactory bulb neurites should not be generalized to other axons. Moreover the mechanisms of action of  $\beta$ -netrin on individual olfactory bulb and retinal neurites await single cell assays (de la Torre et al., 1997; Hong et al., 1999).

It is somewhat perplexing to find that  $\beta$ -netrin and the short arm domains of the laminin  $\gamma$ 2 and  $\gamma$ 3 chains all have similar effects upon axon outgrowth from olfactory bulb explants in vitro. The positive effects of the  $\gamma$ 2 short arms are particularly informative, as  $\gamma$ 2 totally lacks the VI domain and contains only three and one-half EGF-like repeats in domain V. Thus, the  $\gamma$ 2 chain and  $\beta$ -netrin share amino acid identity in only the second and third EGF-like repeats of laminin domain V. These findings strongly suggest that the outgrowth activity of  $\beta$ -netrin and laminins themselves may be mediated by EGF-like repeats within the V domain. In fact, the EGF-like repeat, V-2, is the most highly conserved among the mouse netrins, suggesting that the outgrowth-promoting activity may reside within this region of the molecule. Others have made similar suggestions in *C. elegans* (Wadsworth et al., 1996) and have shown that the Unc 6 molecule contains multifunctional guidance cues; the V-2 domain is important in axon guidance, specifically repelling circumferential axons dorsally. Moreover, the COOH-terminal region is not necessary to rescue the netrin-1 deletion (Lim et al., 1999). The only data that appear to conflict with this model are those provided by the laminin  $\beta$ 2 short arm. It is interesting that, although the  $\beta$ 2 short arm is the fragment with greatest identity to  $\beta$ -netrin, the  $\beta$ 2 short arm has no statistically significant effect on neurite extension or elongation, in contrast to other laminin short arms. This is despite a slight trend towards increased neuritogenesis in treated cultures (Fig. 10 and Table I).

Two final points deserve attention. First, all species of molecules applied in our assay inhibited neurite extension if applied at a high concentration. This suggests that the response of neurons to laminin short arms and the netrins is biphasic; similar data have been reported for netrin-1 (Serafini et al., 1994; Métin et al., 1997). The biphasic response may reflect multiple receptors for these molecules or multiple signal transduction cascade mechanisms. Responses to netrin-1 are complex and can be repulsive as well as attractant for both axons and migrating neurons (Serafini et al., 1994; Colamarino and Tessier-Lavigne, 1995; Wadsworth et al., 1996; Kim et al., 1999; Alcantara et al., 2000). Second, it is worthy to note that  $\beta$ -netrin lacking the C domain has a greater activity in our neurite extension assay on a molar basis than does full-length  $\beta$ -netrin (Table I). This may reflect the observation that full-length, but not truncated  $\beta$ -netrin forms dimers (Fig. 3). In this assay, dimer formation may reduce the apparent activity of  $\beta$ -netrin; further experiments are needed to determine the mechanisms of action of  $\beta$ -netrin. In *C. elegans*, while a truncated form of the netrin-1 molecule (unc6 $\Delta$ C) can rescue the UNC6(-/-) phenotype, it produces aberrant

branching (Lim et al., 1999) which might be related to increased activity of truncated form of  $\beta$ -netrin that we have observed in vitro.

### *$\beta$ -Netrin May Have Significant Roles Outside of the Central Nervous System*

In addition to its expression in the nervous system,  $\beta$ -netrin is deposited around the smooth muscle cells of all somatic muscular arteries, between cardiac myocytes and in the basement membrane of brain capillaries. Together, these data suggest a role for  $\beta$ -netrin in vascular development. Several recent studies document that some molecular species are active in both nervous and vascular development. For example, neuropilin-1, which is a critical axon guidance molecule, has been shown to be a receptor for vascular endothelial growth factor and to be expressed by endothelial cells (Soker et al., 1998). Mice deficient in neuropilin-1 expression demonstrate vascular insufficiency and disorganization. Similarly, the putative neural guidance molecules, the ephs and ephrins, are expressed in the vascular system; ephrin-B2 has been found on the surfaces of arteries but not on veins (Wang et al., 1998) and a complementary expression of its receptor eph-B4 was found on veins but not arteries. These findings support the concept that these neuroactive signaling molecules may be crucial for morphogenesis of the vascular tree. Finally, neural stem cells, presumably fated to generate neurons, are also capable of taking on a smooth muscle cell fate under certain conditions (Tsai and McKay, 2000).

Similarly, it may be that  $\beta$ -netrin functions in both the nervous system and in the vasculature. In both systems, the protein product is present near its site of synthesis, suggesting that in both systems  $\beta$ -netrin is not instructive in either axonal guidance or vascular development but may be permissive, promoting axonal or vascular development. Whereas the functions and mechanisms of action of  $\beta$ -netrin await elucidation, its localization in basement membranes suggests  $\beta$ -netrin may stabilize growing and mature elements, or provide positive growth cues along established axon or vascular highways.

The authors would like to thank Drs. Howard Baden for help with the interdermal injection of rabbits, Fletcher White for the dissection of mouse CNS tissues, and Marie-France Champlaud for advice and direction in the protein extractions.

This work was supported by Public Health Service grants, R01 NS39502 and R37 AR35689 (to R.E. Burgeson) and R01 EY12037 (to D.D. Hunter), the Ziegler Foundation (to W.J. Brunken), and by the Cutaneous Biology Research Center, which is supported, in part, by the MGH/Shiseido Co. Ltd. Agreement.

Submitted: 7 July 2000

Revised: 24 August 2000

Accepted: 25 August 2000

### References

- Alcantara, S., M. Ruiz, F. De Castro, E. Soriano, and C. Sotelo. 2000. Netrin-1 acts as an attractive or as a repulsive cue for distinct migrating neurons during the development of the cerebellar system. *Development*. 127:1359-1372.
- Altschul, S.F., W. Gish, W. Miller, E.W. Myers, and D.J. Lipman. 1990. Basic local alignment search tool. *J. Mol. Biol.* 215:403-410.
- Amano, S., I.C. Scott, K. Takahara, M. Koch, D.R. Gerecke, D.R. Keene, D.L. Hudson, T. Nishiyama, S. Lee, D.S. Greenspan, and R.E. Burgeson. 2000. Bone morphogenetic protein 1 (BMP-1) is an extracellular processing enzyme of the laminin 5  $\gamma$ 2 chain. *J. Biol. Chem.* 275:22728-22735.

- Bashaw, G.J., and C.S. Goodman. 1999. Chimeric axon guidance receptors: the cytoplasmic domains of slit and netrin receptors specify attraction versus repulsion. *Cell*. 97:917–926.
- Boguski, M.S., T.M. Lowe, and C.M. Tolstoshev. 1993. dbEST: database for “expressed sequence tags.” *Nat. Genet.* 4:332–333.
- Colamarino, S.A., and M. Tessier-Lavigne. 1995. The axonal chemoattractant netrin-1 is also a chemorepellent for trochlear motor axons. *Cell*. 81:621–629.
- Deiner, M.S., and D.W. Sretavan. 1999. Altered midline axon pathways and ectopic neurons in the developing hypothalamus of netrin-1 and DCC-deficient mice. *J. Neurosci.* 19:9900–9912.
- Deiner, M.S., T.E. Kennedy, A. Fazeli, T. Serafini, M. Tessier-Lavigne, and D.W. Sretavan. 1997. Netrin-1 and DCC mediate axon guidance locally at the optic disc: loss of function leads to optic nerve hypoplasia. *Neuron*. 19:575–589.
- de la Torre, J.R., V.H. Hopker, G.L. Ming, M.-M. Poo, M. Tessier-Lavigne, A. Hemmati-Brivanlou, and C.E. Holt. 1997. Turning of retinal growth cones in a netrin-1 gradient mediated by the netrin receptor DCC. *Neuron*. 19:1211–1224.
- Goldowitz, D., K.M. Hamre, S.A. Przyborski, and S.L. Ackerman. 2000. Granule cells and cerebellar boundaries: analysis of Unc5h3 mutant chimeras. *J. Neurosci.* 20:4129–4137.
- Harlow, E., and D. Lane. 1988. *Antibodies: A Laboratory Manual*. Cold Spring Harbor Laboratory Press, Cold Spring Harbor, NY. 726 pp.
- Harris, R., L.M. Sabatelli, and M.A. Seeger. 1996. Guidance cues at the *Drosophila* CNS midline: identification and characterization of two *Drosophila* Netrin/UNC-6 homologs. *Neuron*. 17:217–228.
- Hedgecock, E.M., J.G. Culotti, and D.H. Hall. 1990. The unc-5, unc-6, and unc-40 genes guide circumferential migrations of pioneer axons and mesodermal cells on the epidermis in *C. elegans*. *Neuron*. 4:61–85.
- Hong, K., L. Hinck, M. Nishiyama, M.-M. Poo, M. Tessier-Lavigne, and E. Stein. 1999. A ligand-gated association between cytoplasmic domains of UNC5 and DCC family receptors converts netrin-induced growth cone attraction to repulsion. *Cell*. 97:927–941.
- Hunter, D.D., V. Shah, J.P. Merlie, and J.R. Sanes. 1989. A laminin-like adhesive protein concentrated in the synaptic cleft of the neuromuscular junction. *Nature*. 338:229–234.
- Ishii, N., W.G. Wadsworth, B.D. Stern, J.G. Culotti, and E.M. Hedgecock. 1992. UNC-6, a laminin-related protein, guides cell and pioneer axon migrations in *C. elegans*. *Neuron*. 9:873–881.
- Keino-Masu, K., M. Masu, L. Hinck, E.D. Leonardo, S.S. Chan, J.G. Culotti, and M. Tessier-Lavigne. 1996. Deleted in colorectal cancer (DCC) encodes a netrin receptor. *Cell*. 87:175–185.
- Kennedy, T.E., T. Serafini, J.R. de la Torre, and M. Tessier-Lavigne. 1994. Netrins are diffusible chemotropic factors for commissural axons in the embryonic spinal cord. *Cell*. 78:425–435.
- Kim, S., and W.G. Wadsworth. 2000. Positioning of longitudinal nerves in *C. elegans* by nidogen. *Science*. 288:150–154.
- Kim, S., X.C. Ren, E. Fox, and W.G. Wadsworth. 1999. SDQR migrations in *Caenorhabditis elegans* are controlled by multiple guidance cues and changing responses to netrin UNC-6. *Development*. 126:3881–3890.
- Koch, M., P. Olsen, A. Albus, W. Jin, D.D. Hunter, W.J. Brunken, R.E. Burgeson, and M.-F. Champlaud. 1999. Characterization and expression of the laminin  $\gamma$ 3 chain: a novel, non-basement membrane, associated laminin chain. *J. Cell Biol.* 145:605–617.
- Laemmli, U.K. 1970. Cleavage of structural proteins during the assembly of the head of bacteriophage T4. *Nature*. 227:680–685.
- Lauderdale, J.D., N.M. Davis, and J.Y. Kuwada. 1997. Axon tracts correlate with netrin-1a expression in the zebrafish embryo. *Mol. Cell. Neurosci.* 9:293–313.
- Li, H., J. Chen, W. Wu, T. Fagaly, L. Zhou, W. Yuan, S. Dupuis, Z. Jiang, W. Nash, C. Gick, D.M. Ornitz, J.Y. Wu, and Y. Rao. 1999. Vertebrate slit, a secreted ligand for the transmembrane protein roundabout, is a repellent for olfactory bulb axons. *Cell*. 96:807–818.
- Libby, R.T., Y. Xu, L.M. Selfors, W.J. Brunken, and D.D. Hunter. 1997. Identification of the cellular source of laminin  $\beta$ 2 in the adult and developing vertebrate retina. *J. Comp. Neurol.* 389:355–367.
- Lim Y.S., S. Mallapur, G. Kao, X.C. Ren, and W.G. Wadsworth. 1999. Netrin UNC-6 and the regulation of branching and extension of motoneuron axons from the ventral nerve cord of *Caenorhabditis elegans*. *J. Neurosci.* 19:7048–7056.
- Lunstrum, G.P., L.Y. Sakai, D.R. Keene, N.P. Morris, and R.E. Burgeson. 1986. Large complex globular domains of type VII procollagen contribute to the structure of anchoring fibrils. *J. Biol. Chem.* 261:9042–9048.
- MacLennan, A.J., D.L. McLaurin, L. Marks, E.N. Vinson, M. Pfeifer, S.V. Zulf, M.B. Heaton, and N. Lee. 1997. Immunohistochemical localization of netrin-1 in the embryonic chick nervous system. *J. Neurosci.* 17:5466–5479.
- Métin, C., D. Deléglise, T. Serafini, T.E. Kennedy, and M. Tessier-Lavigne. 1997. A role for netrin-1 in the guidance of cortical efferents. *Development*. 124:5063–5074.
- Meyerhardt, J.A., K. Caca, B.C. Eckstrand, G. Hu, C. Lengauer, S. Banavali, A.T. Look, and E.R. Fearon. 1999. Netrin-1: interaction with deleted in colorectal cancer (DCC) and alterations in brain tumors and neuroblastomas. *Cell Growth Differ.* 10:35–42.
- Mitchell, K.J., J.L. Doyle, T. Serafini, T.E. Kennedy, M. Tessier-Lavigne, C.S. Goodman, and B.J. Dickson. 1996. Genetic analysis of Netrin genes in *Drosophila*: netrins guide CNS commissural axons and peripheral motor axons. *Neuron*. 17:203–215.
- Murrell, J.R., and D.D. Hunter. 1999. An olfactory sensory neuron line, *odora*, properly targets olfactory proteins and responds to odorants. *J. Neurosci.* 19:8260–8270.
- Nielsen, H., J. Engelbrecht, S. Brunak, and G. von Heijne. 1997. Identification of prokaryotic and eukaryotic signal peptides and prediction of their cleavage sites. *Protein Eng.* 10:1–6.
- Pini, A. 1993. Chemorepulsion of axons in the developing mammalian central nervous system. *Science*. 261:95–98.
- Przyborski, S.A., B.B. Knowles, and S.L. Ackerman. 1998. Embryonic phenotype of Unc5h3 mutant mice suggests chemorepulsion during the formation of the rostral cerebellar boundary. *Development*. 125:41–50.
- Puschel, A.W. 1999. Divergent properties of mouse netrins. *Mech. Dev.* 83:65–75.
- Rousselle, P., D.R. Keene, F. Ruggiero, M.-F. Champlaud, M. van der Rest, and R.E. Burgeson. 1997. Laminin 5 binds the NC-1 domain of type VII collagen. *J. Cell Biol.* 138:719–728.
- Serafini, T., T.E. Kennedy, M.J. Galko, C. Mirzayan, T.M. Jessell, and M. Tessier-Lavigne. 1994. The netrins define a family of axon outgrowth-promoting proteins homologous to *C. elegans* UNC-6. *Cell*. 78:409–424.
- Serafini, T., S.A. Colamarino, E.D. Leonardo, H. Wang, R. Beddington, W.C. Skarnes, and M. Tessier-Lavigne. 1996. Netrin-1 is required for commissural axon guidance in the developing vertebrate nervous system. *Cell*. 87:1001–1014.
- Skarnes, W.C., J.E. Moss, S.M. Hurtley, and R.S. Beddington. 1995. Capturing genes encoding membrane and secreted proteins important for mouse development. *Proc. Natl. Acad. Sci. USA*. 92:6592–6596.
- Soker, S., S. Takashima, H.Q. Miao, G. Neufeld, and M. Klagsbrun. 1998. Neuropilin-1 is expressed by endothelial and tumor cells as an isoform-specific receptor for vascular endothelial growth factor. *Cell*. 92:735–745.
- Strahle, U., N. Fischer, and P. Blader. 1997. Expression and regulation of a netrin homologue in the zebrafish embryo. *Mech. Dev.* 62:147–160.
- Tsai, R.Y.L., and R.D.G. McKay. 2000. Cell contact regulates fate choice by cortical stem cells. *J. Neurosci.* 20:3725–3735.
- Van Raay, T.J., S.M. Foskett, T.D. Connors, K.W. Klinger, G.M. Landes, and T.C. Burn. 1997. The NTN2L gene encoding a novel human netrin maps to the autosomal dominant polycystic kidney disease region on chromosome 16p13.3. *Genomics*. 41:279–282.
- Wadsworth, W.G., H. Bhatt, and E.M. Hedgecock. 1996. Neuroglia and pioneer neurons express UNC-6 to provide global and local netrin cues for guiding migrations in *C. elegans*. *Neuron*. 16:35–46.
- Walsh, C.A., and A.M. Goffinet. 2000. Potential mechanisms of mutations that affect neuronal migration in man and mouse. *Curr. Opin. Genet. Dev.* 10:270–274.
- Wang, H., N.G. Copeland, D.J. Gilbert, N.A. Jenkins, and M. Tessier-Lavigne. 1999. Netrin-3, a mouse homolog of human NTN2L, is highly expressed in sensory ganglia and shows differential binding to netrin receptors. *J. Neurosci.* 19:4938–4947.
- Wang, H.U., Z.-F. Chen., and D.F. Anderson. 1998. Molecular distinction and angiogenic interaction between embryonic arteries and veins revealed by ephrin-B2 and its receptor Eph-B4. *Cell*. 93:741–753.
- Whitaker, J.R., and P.E. Granum. 1980. An absolute method for protein determination based on difference in absorbance at 235 and 280 nm. *Anal. Biochem.* 109:156–159.
- Winberg, M.L., K.J. Mitchell, and C.S. Goodman. 1998. Genetic analysis of the mechanisms controlling target selection: complementary and combinatorial functions of netrins, semaphorins, and IgCAMs. *Cell*. 93:581–591.
- Yee, K.T., H.H. Simon, M. Tessier-Lavigne, and D.D.M. O’Leary. 1999. Extension of long leading processes and neuronal migration in the mammalian brain directed by the chemoattractant netrin-1. *Neuron*. 24:607–622.